

LHeC Detector Design



LHeC:
 $E_e = 60$ GeV
 $E_p = 7$ TeV

CDR design 2012

Detector now including FCC-he

Tracker and Calorimeters

Project Development – Next Steps

For references,
please consult
lhec.web.cern.ch

LHeC CDR
[arXiv:1206.2913](https://arxiv.org/abs/1206.2913)
J.Phys. G39 (2012) 075001

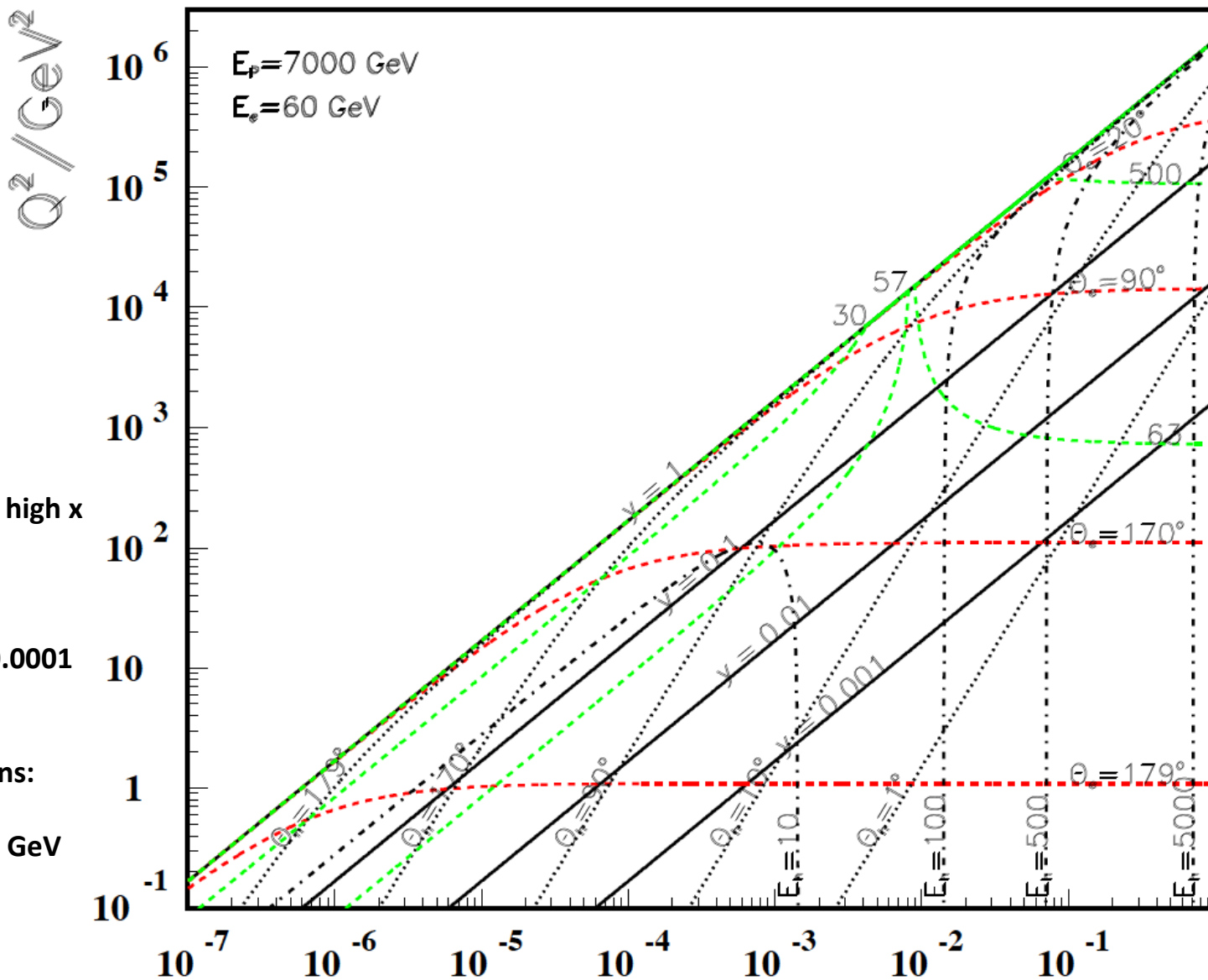
Max Klein
University of Liverpool

for the LHeC Study Group



FCC_eh:
 $E_e = 60$ GeV
 $E_p = 50$ TeV

HE LHC:
 $E_p = 14$ TeV



Observations

Good angular coverage but at high x low Q^2

High Q^2 to 10^6
CC at large $x > 0.0001$

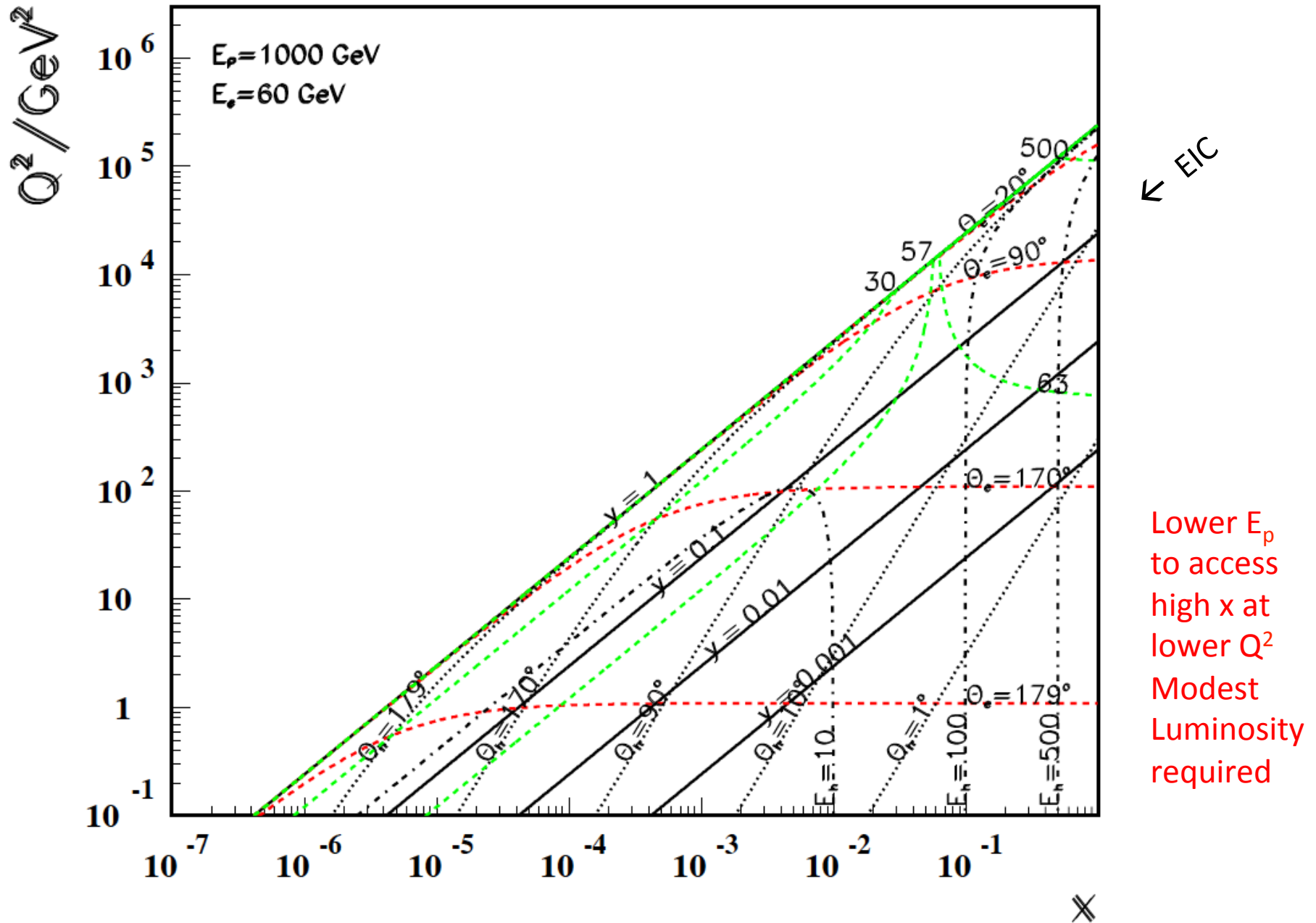
Low Q^2 High x
Very fwd hadrons:

High $y = 0.9 \rightarrow 6 \text{ GeV}$
 F_L "easy"



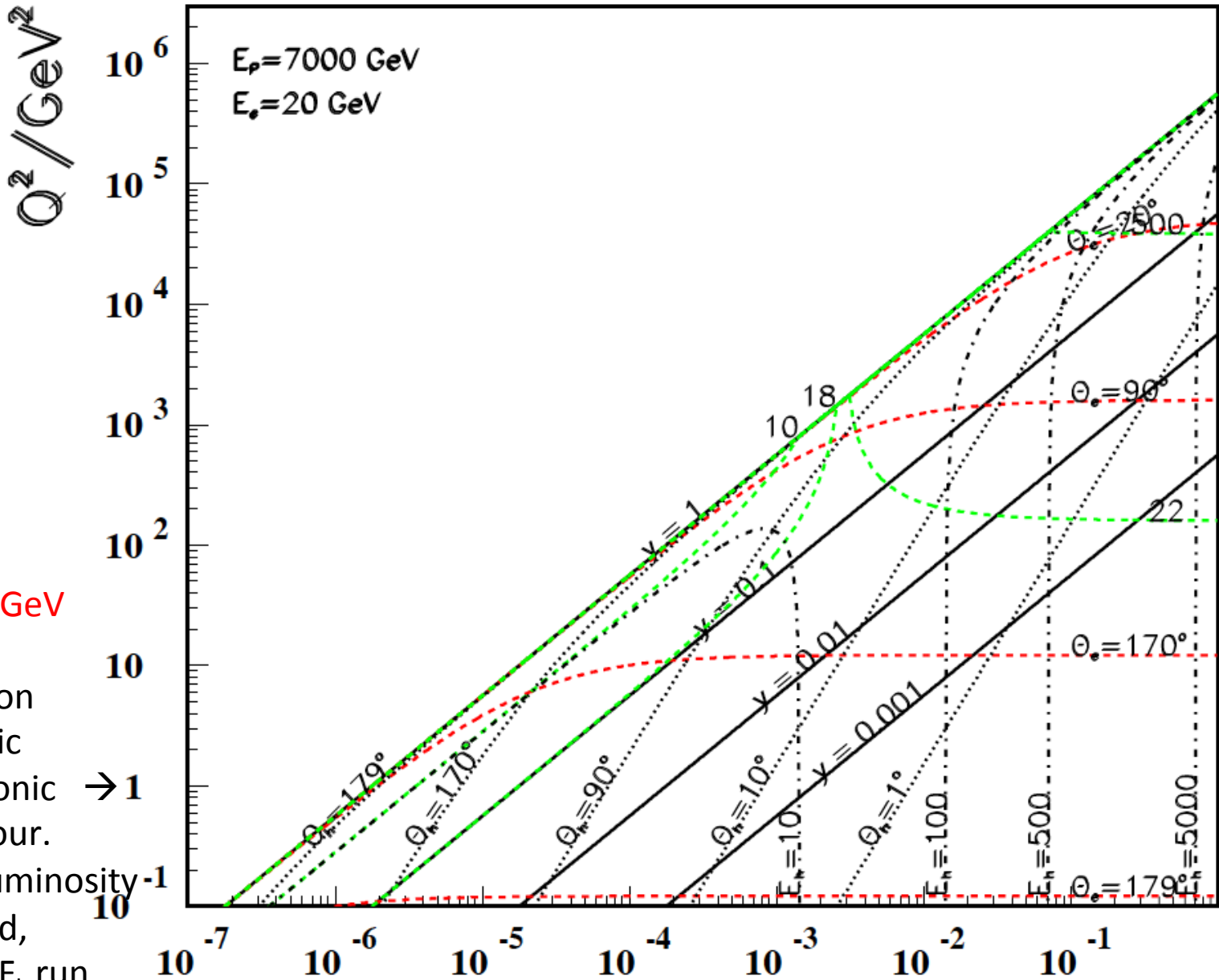
Kinematics at LHeC

Lower proton energy



Kinematics at LHeC

Lower electron energy



$E_e = 20 \text{ GeV}$

Covers transition hadronic to partonic behaviour. $\rightarrow 1$

“NO” luminosity required, part of F_L run



NC Cross Section Correlated Uncertainties ($Q^2=2 \text{ GeV}^2$)

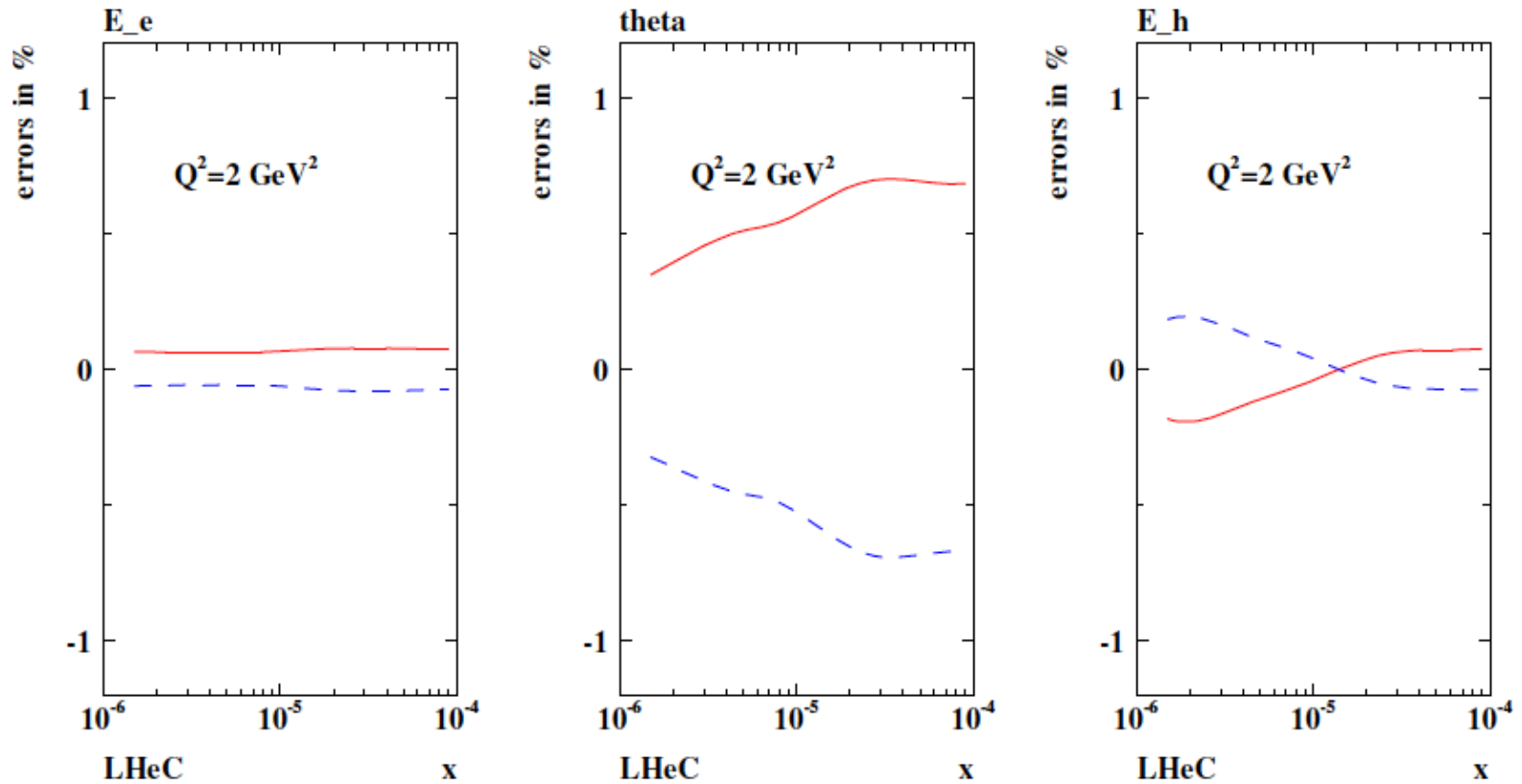


Figure 3.2: Neutral current cross section errors, calculated for $60 \times 7000 \text{ GeV}^2$, resulting from scale uncertainties of the scattered electron energy $\delta E'_e/E'_e = 0.1 \%$, of its polar angle $\delta\theta_e = 0.1 \text{ mrad}$ and the hadronic final state energy $\delta E_h/E_h = 0.5 \%$, at low $Q^2 = 2 \text{ GeV}^2$ and correspondingly low x .

NC Cross Section Correlated Uncertainties ($Q^2=20000 \text{ GeV}^2$)

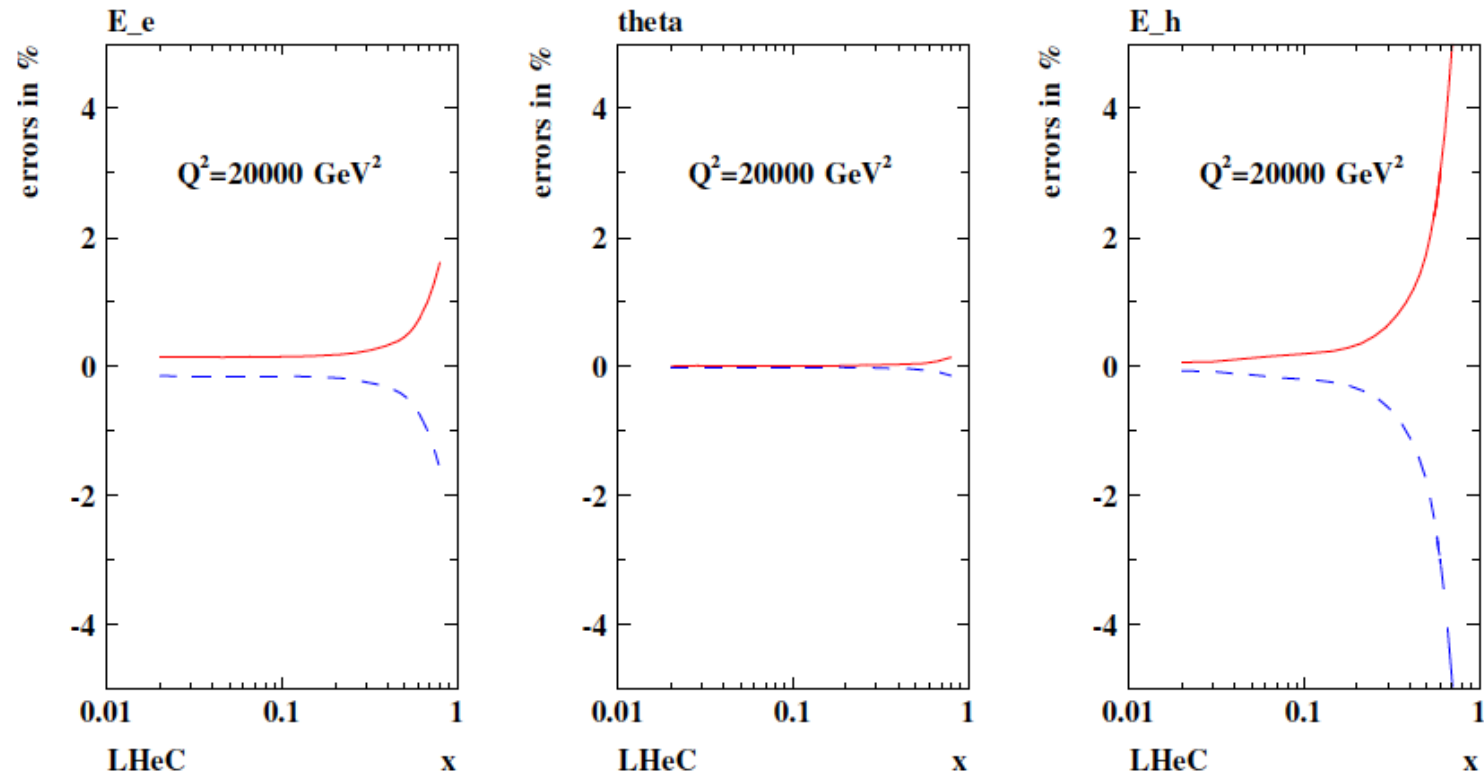


Figure 3.3: Neutral current cross section errors, calculated for $60 \times 7000 \text{ GeV}^2$ unpolarised e^-p scattering, resulting from scale uncertainties of the scattered electron energy $\delta E'_e/E'_e = 0.1\%$, of its polar angle $\delta\theta_e = 0.1 \text{ mrad}$ and the hadronic final state energy $\delta E_h/E_h = 0.5\%$, at large $Q^2 = 20000 \text{ GeV}^2$ and correspondingly large x . Note that the characteristic behaviour of the relative uncertainty at large x , i.e. to diverge $\propto 1/(1-x)$, is independent of Q^2 , i.e. persistently observed at $Q^2 = 200000 \text{ GeV}^2$ for example too.

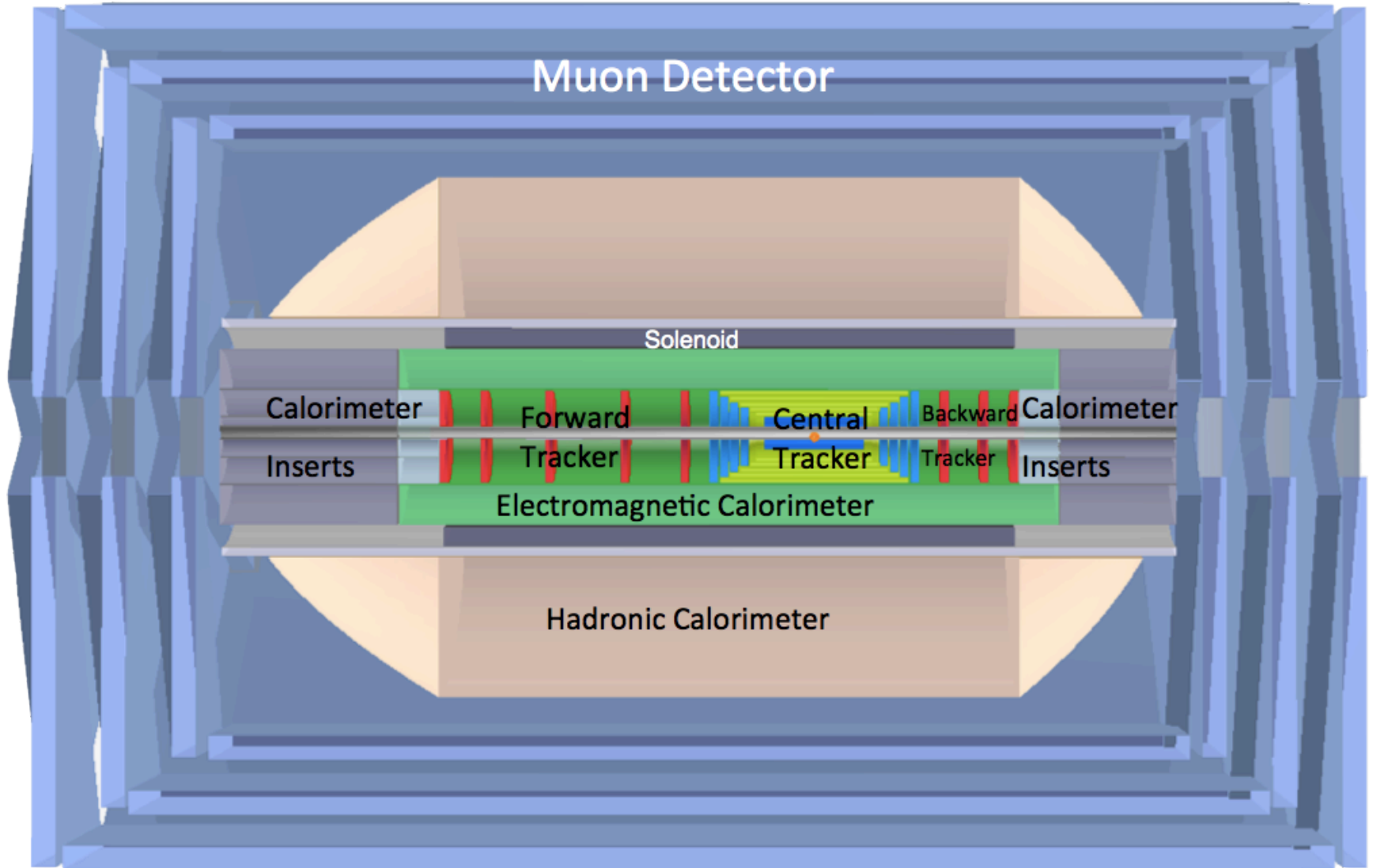
Detector in the CDR

kinematics and requirements

region of detector	backward	barrel	forward
approximate angular range / degrees	179 - 135	135 -45	45-1
scattered electron energy/GeV	3-100	10-400	50-5000
x_e	$10^{-7} - 1$	$10^{-4} - 1$	$10^{-2} - 1$
elm scale calibration in %	0.1	0.2	0.5
elm energy resolution $\delta E/E$ in % $\cdot \sqrt{E/GeV}$	10	15	15
hadronic final state energy/GeV	3-100	3-200	3-5000
x_h	$10^{-7} - 10^{-3}$	$10^{-5} - 10^{-2}$	$10^{-4} - 1$
hadronic scale calibration in %	2	1	1
hadronic energy resolution in % $\cdot \sqrt{E/GeV}$	60	50	40

Now: Higgs: maximum fwd acceptance (p direction), better hadronic resolution, crucial c and b tagging capabilities. Still muon tag only (but muon momentum for FCC-eh for H)

LHeC Detector in the CDR (2012)

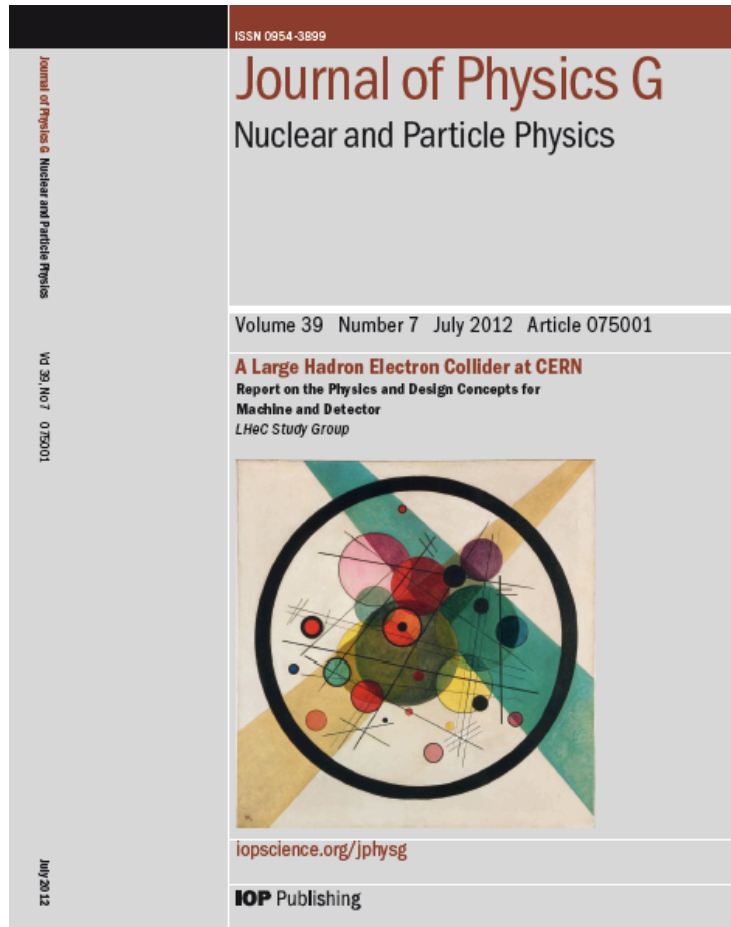


Forward/backward asymmetry in energy deposited and thus in geometry and technology

Present dimensions: $L \times D = 14 \times 9 \text{ m}^2$ [CMS $21 \times 15 \text{ m}^2$, ATLAS $45 \times 25 \text{ m}^2$]

Taggers at -62 m (e), 100 m (γ, LR), -22.4 m (γ, RR), $+100 \text{ m}$ (n), $+420 \text{ m}$ (p)

Design Report 2012



arXiv:1206.2913

CERN Referees

Ring Ring Design

Kurt Huebner (CERN)
Alexander N. Skrinsky (INP Novosibirsk)
Ferdinand Willeke (BNL)

Linac Ring Design

Reinhard Brinkmann (DESY)
Andy Wolski (Cockcroft)
Kaoru Yokoya (KEK)

Energy Recovery

Georg Hoffstaetter (Cornell)
Ilan Ben Zvi (BNL)

Magnets

Neil Marks (Cockcroft)
Martin Wilson (CERN)

Interaction Region

Daniel Pitzl (DESY)
Mike Sullivan (SLAC)

Detector Design

Philippe Bloch (CERN)
Roland Horisberger (PSI)

Installation and Infrastructure

Sylvain Weisz (CERN)

New Physics at Large Scales

Cristinel Diaconu (IN2P3 Marseille)
Gian Giudice (CERN)

Michelangelo Mangano (CERN)

Precision QCD and Electroweak

Guido Altarelli (Roma)
Vladimir Chekelian (MPI Munich)
Alan Martin (Durham)

Physics at High Parton Densities

Alfred Mueller (Columbia)
Raju Venugopalan (BNL)
Michele Arneodo (INFN Torino)

600 pages. Physics, Detector and Two Accelerator Options

ring-ring which may be of interest in the HE-LHC context and linac-ring, the default LH(e)C

LHeC Study Group

J.L.Abelleira Fernandez^{16,23}, C.Adolphsen⁵⁷, A.N.Akay⁰³, H.Aksakal³⁹, J.L.Albacete⁵², S.Alekhin^{17,54}, P.Allport²⁴, V.Andreev³⁴, R.B.Appleby^{14,30}, E.Arikan³⁹, N.Armento^{53,a}, G.Azelos^{33,64}, M.Bai³⁷, D.Barber^{14,17,24}, J.Bartels¹⁸, O.Behnke¹⁷, J.Behr¹⁷, A.S.Belyaev^{15,56}, I.Ben-Zvi³⁷, N.Bernard²⁵, S.Bertolucci¹⁶, S.Bettoni¹⁶, S.Biswal⁴¹, J.Blümlein¹⁷, H.Böttcher¹⁷, A.Bogacz³⁶, C.Bracco¹⁶, G.Brandt⁴⁴, H.Braun⁶⁵, S.Brodsky^{57,b}, O.Brüning¹⁶, E.Bulyak¹², A.Buniatyan¹⁷, H.Burkhardt¹⁶, I.T.Cakir⁰², O.Cakir⁰¹, R.Calaga¹⁶, V.Cetinkaya⁰¹, E.Ciapala¹⁶, R.Ciftci⁰¹, A.K.Ciftci⁰¹, B.A.Cole³⁸, J.C.Collins⁴⁸, O.Dadoun⁴², J.Dainton²⁴, A.De.Roeck¹⁶, D.d'Enterria¹⁶, A.Dudarev¹⁶, A.Eide⁶⁰, R.Enberg⁶³, E.Eroglu⁶², K.J.Eskola²¹, L.Favart⁰⁸, M.Fitterer¹⁶, S.Forte³², A.Gaddi¹⁶, P.Gambino⁵⁹, H.García Morales¹⁶, T.Gehrmann⁶⁹, P.Gladkikh¹², C.Glasman²⁸, R.Godbole³⁵, B.Goddard¹⁶, T.Greenshaw²⁴, A.Guffanti¹³, V.Guzey^{19,36}, C.Gwenlan⁴⁴, T.Han⁵⁰, Y.Hao³⁷, F.Haug¹⁶, W.Herr¹⁶, A.Hervé²⁷, B.J.Holzer¹⁶, M.Ishitsuka⁵⁸, M.Jacquet⁴², B.Jeanneret¹⁶, J.M.Jimenez¹⁶, J.M.Jowett¹⁶, H.Jung¹⁷, H.Karadeniz⁰², D.Kayran³⁷, A.Kilic⁶², K.Kimura⁵⁸, M.Klein²⁴, U.Klein²⁴, T.Kluge²⁴, F.Kocak⁶², M.Korostelev²⁴, A.Kosmicki¹⁶, P.Kostka¹⁷, H.Kowalski¹⁷, G.Kramer¹⁸, D.Kuchler¹⁶, M.Kuze⁵⁸, T.Lappi^{21,c}, P.Laycock²⁴, E.Levichev⁴⁰, S.Levonian¹⁷, V.N.Litvinenko³⁷, A.Lombardi¹⁶, J.Maeda⁵⁸, C.Marquet¹⁶, B.Mellado²⁷, K.H.Mess¹⁶, A.Milanese¹⁶, S.Moch¹⁷, I.I.Morozov⁴⁰, Y.Muttoni¹⁶, S.Myers¹⁶, S.Nandi⁵⁵, Z.Nergiz³⁹, P.R.Newman⁰⁶, T.Omori⁶¹, J.Osborne¹⁶, E.Paoloni⁴⁹, Y.Papaphilippou¹⁶, C.Pascaud⁴², H.Paukkunen⁵³, E.Perez¹⁶, T.Pieloni²³, E.Pilicer⁶², B.Pire⁴⁵, R.Placakyte¹⁷, A.Polini⁰⁷, V.Ptitsyn³⁷, Y.Pupkov⁴⁰, V.Radescu¹⁷, S.Raychaudhuri³⁵, L.Rinolfi¹⁶, R.Rohini³⁵, J.Rojo^{16,31}, S.Russenschuck¹⁶, M.Sahin⁰³, C.A.Salgado^{53,a}, K.Sampegi⁵⁸, R.Sassot⁰⁹, E.Sauvan⁰⁴, U.Schneekloth¹⁷, T.Schörner-Sadenius¹⁷, D.Schulte¹⁶, A.Senol²², A.Seryi⁴⁴, P.Sievers¹⁶, A.N.Skrinsky⁴⁰, W.Smith²⁷, H.Spiesberger²⁹, A.M.Stasto^{48,d}, M.Strikman⁴⁸, M.Sullivan⁵⁷, S.Sultansoy^{03,e}, Y.P.Sun⁵⁷, B.Surrow¹¹, L.Szymanowski^{66,f}, P.Taels⁰⁵, I.Tapan⁶², T.Tasci²², E.Tassi¹⁰, H.Ten.Kate¹⁶, J.Terron²⁸, H.Thiesen¹⁶, L.Thompson^{14,30}, K.Tokushuku⁶¹, R.Tomás García¹⁶, D.Tommasini¹⁶, D.Trbojevic³⁷, N.Tsoupas³⁷, J.Tuckmantel¹⁶, S.Turkoz⁰¹, T.N.Trinh⁴⁷, K.Tywoniuk²⁶, G.Unel²⁰, J.Urakawa⁶¹, P.VanMechelen⁰⁵, A.Variola⁵², R.Veness¹⁶, A.Vivoli¹⁶, P.Vobly⁴⁰, J.Wagner⁶⁶, R.Wallny⁶⁸, S.Wallon^{43,46,f}, G.Watt¹⁶, C.Weiss³⁶, U.A.Wiedemann¹⁶, U.Wienands⁵⁷, F.Willeke³⁷, B.-W.Xiao⁴⁸, V.Yakimenko³⁷, A.F.Zarnecki⁶⁷, Z.Zhang⁴², F.Zimmermann¹⁶, R.Zlebcik⁵¹, F.Zomer⁴²

11 Detector Requirements	482	13 Forward and Backward Detectors	561
11.1 Cost and magnets	483	13.1 Luminosity measurement and electron tagging	561
11.2 Detector acceptance	484	13.1.1 Options	562
11.2.1 Kinematic reconstruction	484	13.1.2 Use of the main LHeC detector	562
11.2.2 Acceptance for the scattered electron	485	13.1.3 Dedicated luminosity detectors in the tunnel	563
11.2.3 Acceptance for the hadronic final state	487	13.1.4 Small angle electron tagger	564
11.2.4 Acceptance at the High Energy LHC	489	13.1.5 Summary and open questions	566
11.2.5 Energy resolution and calibration	491	13.2 Polarimeter	567
11.2.6 Tracking requirements	492	13.2.1 Polarisation from the scattered photons	568
11.2.7 Particle identification requirements	495	13.2.2 Polarisation from the scattered electrons	569
11.3 Summary of the requirements on the LHeC detector	495	13.3 Zero degree calorimeter	569
12 Central Detector	497	13.3.1 ZDC detector design	569
12.1 Basic detector description	497	13.3.2 Neutron calorimeter	569
12.1.1 Baseline detector layout	503	13.3.3 Proton calorimeter	570
12.1.2 An alternative solenoid placement - option B	505	13.3.4 Calibration and monitoring	571
12.2 Magnet design	507	13.4 Forward proton detection	571
12.2.1 Magnets configuration	507	14 Detector Assembly and Integration	577
12.2.2 Detector solenoid	507	14.1 Detector assembly on surface	578
12.2.3 Detector integrated e-beam bending dipoles	511	14.2 Detector lowering and integration underground	578
12.2.4 Cryogenics for magnets and calorimeter	512	14.3 Maintenance and opening scenario	579
12.3 Tracking detector	514	14.4 Timelines	579
12.3.1 Tracking Detector - Baseline Layout	515		
12.3.2 Performance	516		
12.3.3 Tracking detector design criteria and possible solutions	519		
12.4 Calorimetry	524		
12.4.1 The barrel electromagnetic calorimeter	525		
12.4.2 The hadronic barrel calorimeter	526		
12.4.3 Endcap calorimeters	529		
12.5 Calorimeter simulation	529		
12.5.1 The barrel LAr calorimeter simulation	530		
12.5.2 The barrel tile calorimeter simulation	531		
12.5.3 Combined liquid argon and tile calorimeter simulation	533		
12.5.4 Lead-Scintillator electromagnetic option	533		
12.5.5 Forward and backward inserts calorimeter simulation	537		
12.6 Calorimeter summary	545		
12.7 Muon detector	546		
12.7.1 Muon detector design	547		
12.7.2 The LHeC muon detector options	549		
12.7.3 Forward muon extensions	550		
12.7.4 Muon detector summary	551		
12.8 Event and detector simulations	553		
12.8.1 Pythia6	553		
12.8.2 1 MeV neutron equivalent	554		
12.8.3 Nearest neighbour	555		
12.8.4 Cross checking	558		
12.8.5 Future goals	560		



LHeC Detector in the CDR (1206.2913)

Detector Magnets

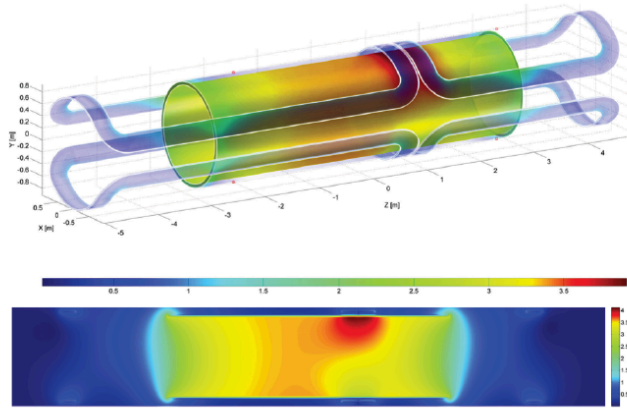


Figure 13.13: Magnetic field of the magnet system of solenoid and the two internal superconducting dipoles at nominal currents (effect of iron ignored). The position of the peak magnetic field of 3.9 T is local due to the adjacent current return heads on top of the solenoid where all magnetic fields add up.

Dipole (for head on LR) and solenoid in common cryostat, perhaps with electromagnetic LAr

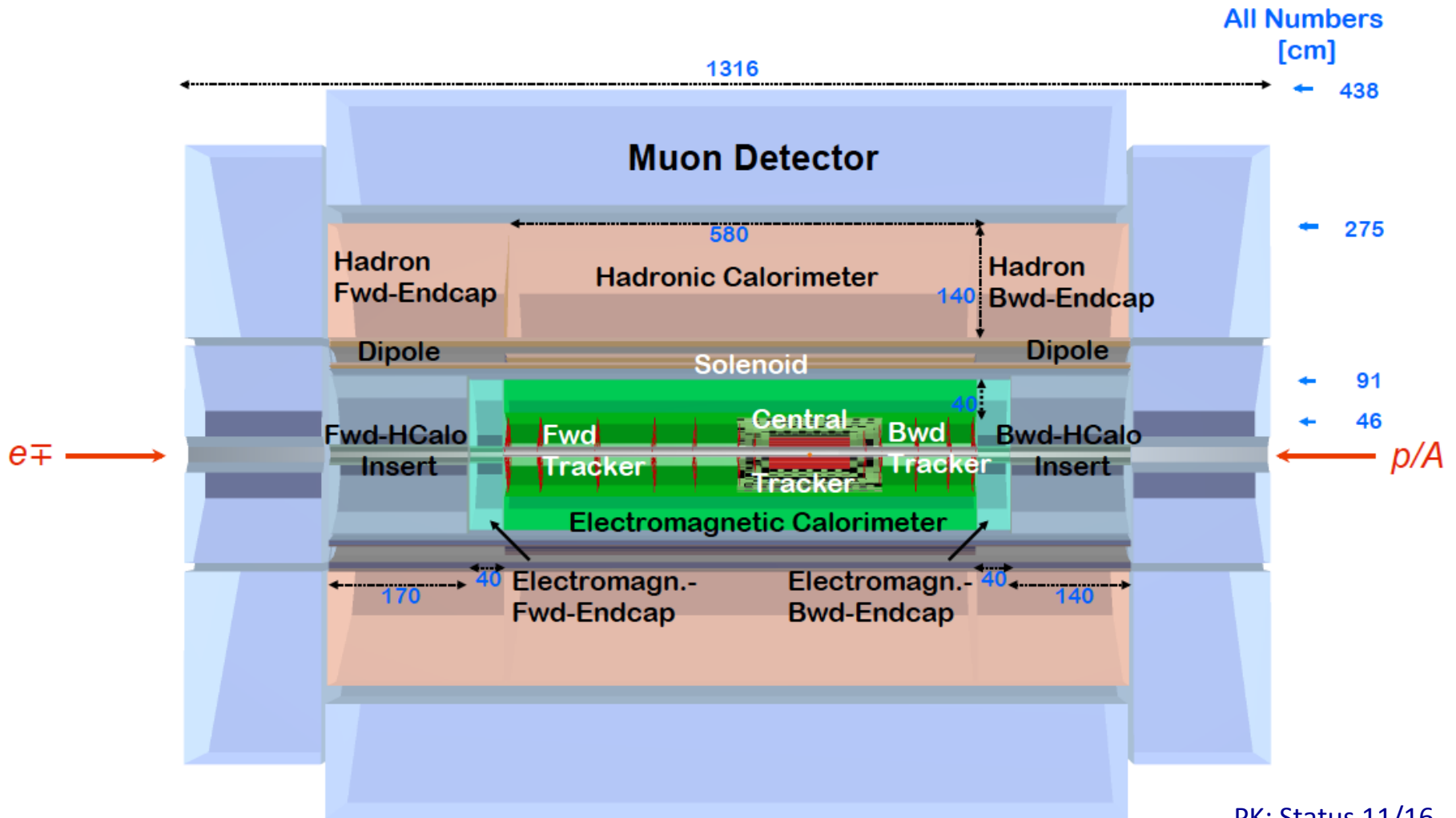
3.5T field at ~1m radius to house a Silicon tracker

Based on ATLAS+CMS experience

Property	Parameter	value	unit
Dimensions	Cryostat inner radius	0.900	m
	Length	10.000	m
	Outer radius	1.140	m
	Coil windings inner radius	0.960	m
	Length	5.700	m
	Thickness	60.0	mm
	Support cylinder thickness	0.030	m
	Conductor section, Al-stabilized NbTi/Cu + insulation	30.0 × 6.8	mm ²
	Length	10.8	km
	Superconducting cable section, 20 strands	12.4 × 2.4	mm ²
	Superconducting strand diameter Cu/NbTi ratio = 1.25	1.24	mm
	Masses	Conductor windings	5.7
Support cylinder, solenoid section + dipole sections		5.6	t
Total cold mass		12.8	t
Cryostat including thermal shield		11.2	t
Electro-magnetics	Total mass of cryostat, solenoid and small parts	24	t
	Central magnetic field	3.50	T
	Peak magnetic field in windings (dipoles off)	3.53	T
	Peak magnetic field in solenoid windings (dipoles on)	3.9	T
	Nominal current	10.0	kA
	Number of turns, 2 layers	1683	
	Self-inductance	1.7	H
	Stored energy	82	MJ
	E/m, energy-to-mass ratio of windings	14.2	kJ/kg
	E/m, energy-to-mass ratio of cold mass	9.2	kJ/kg
	Charging time	1.0	hour
	Current rate	2.8	A/s
Margins	Inductive charging voltage	2.3	V
	Coil operating point, nominal / critical current	0.3	
	Temperature margin at 4.6 K operating temperature	2.0	K
Mechanics	Cold mass temperature at quench (no extraction)	~ 80	K
	Mean hoop stress	~ 55	MPa
Cryogenics	Peak stress	~ 85	MPa
	Thermal load at 4.6 K, coil with 50% margin	~ 110	W
	Radiation shield load width 50% margin	~ 650	W
	Cooling down time / quench recovery time	4 and 1	day
	Use of liquid helium	~ 1.5	g/s

Table 13.1: Main parameters of the baseline LHeC Solenoid providing 3.5 T in a free bore of 1.8 m.

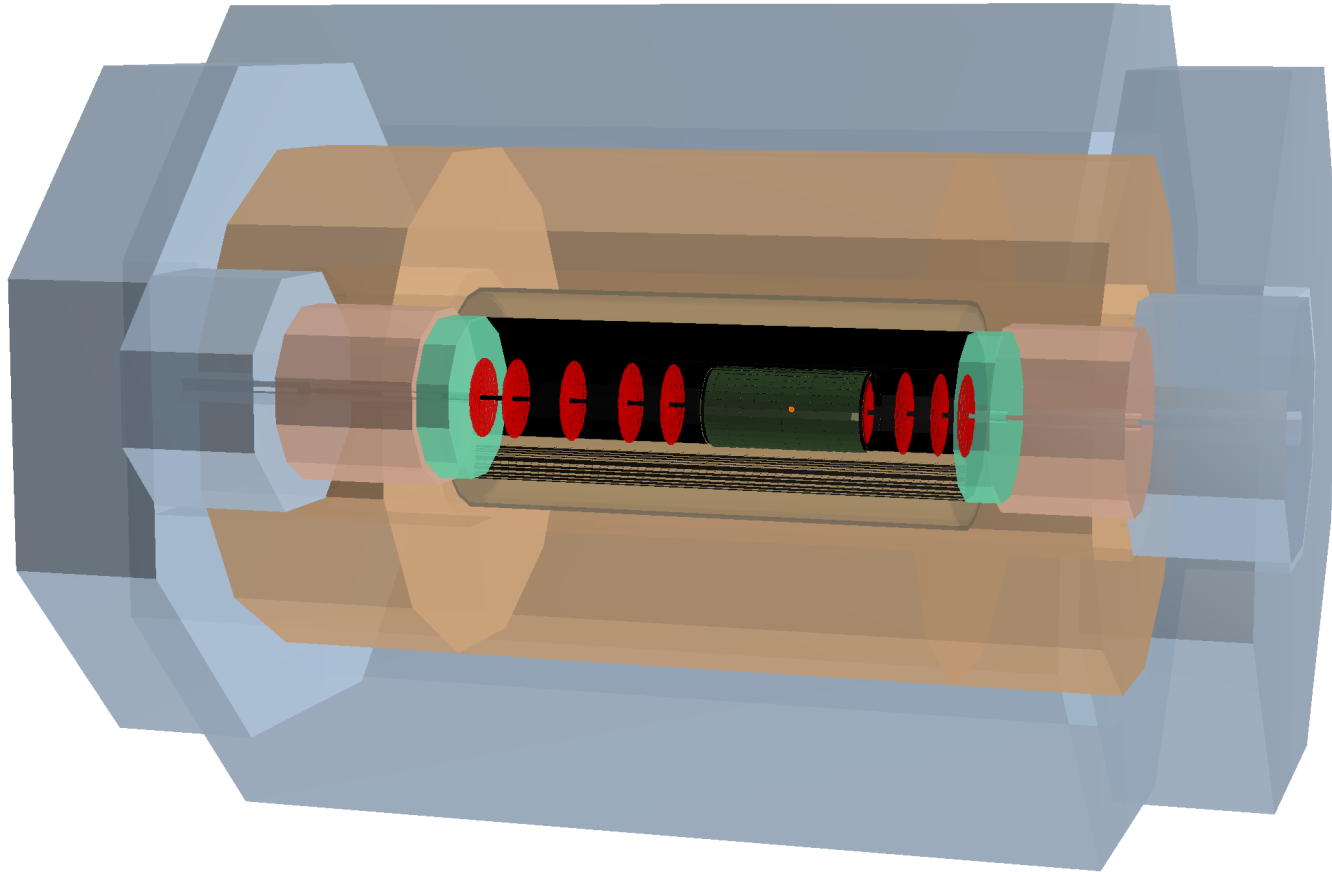
LHeC Detector 2016



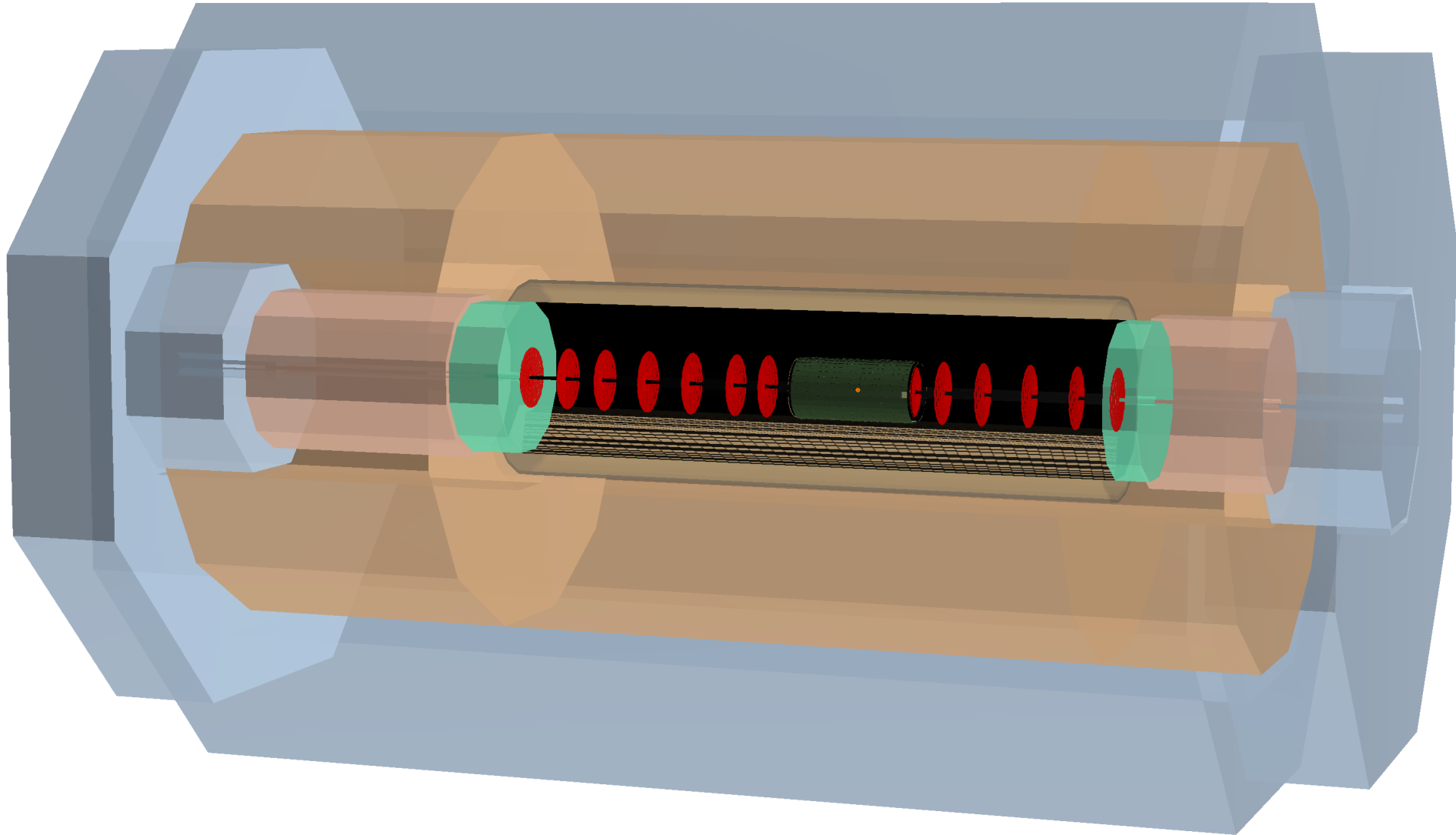
Dimensions and Multitudes - LHeC

Tracker	FST _{pix}	FST _{striz}	CFT _{pix}	CPT _{pix}	CST _{striz}	CBT _{pix}	BST _{striz}	BST _{pix}
#Wheels	5		2	–	–	2	3	
#Rings/Wheel	2 _{inner}	3 _{outer}	3/4	–	–	3/4	3 _{outer}	2 _{inner}
#Layers	–	–	–	4	5	–	–	–
$\theta_{min/max}$ [°]	0.7	3.8	3.0	5.1	24/155	177.8	173.1	178.7
$\eta_{max/min}$	5.1	3.4	3.6	±3.1	±1.4	-3.6	-2.8	-4.5
Si _{pix/striz} [m ²]	6.9	9.5	2.8	5.4	33.7	2.8	5.7	4.1
Sum-Si [m ²]	70.9 double layers taken into account							
Calo	FHC _{SiW}	FEC _{SiW}	EMC _{SciPb/LAr}		HAC _{SciFe}		BEC _{SiPb}	BHC _{SiFe}
$\theta_{min/max}$ [°]	0.61	0.68	8/166		14.2/160		178.7	178.9
$\eta_{max/min}$	5.2	5.1	2.7/-2.1		2.1/-1.7		-4.5	-4.7
Volume [m ³]	6.7	1.6	15.1		165		1.6	5.8
Sum-Si [m ²]	197.4							

LHeC Detector



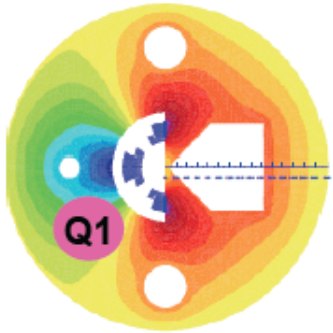
FCC-eh Detector



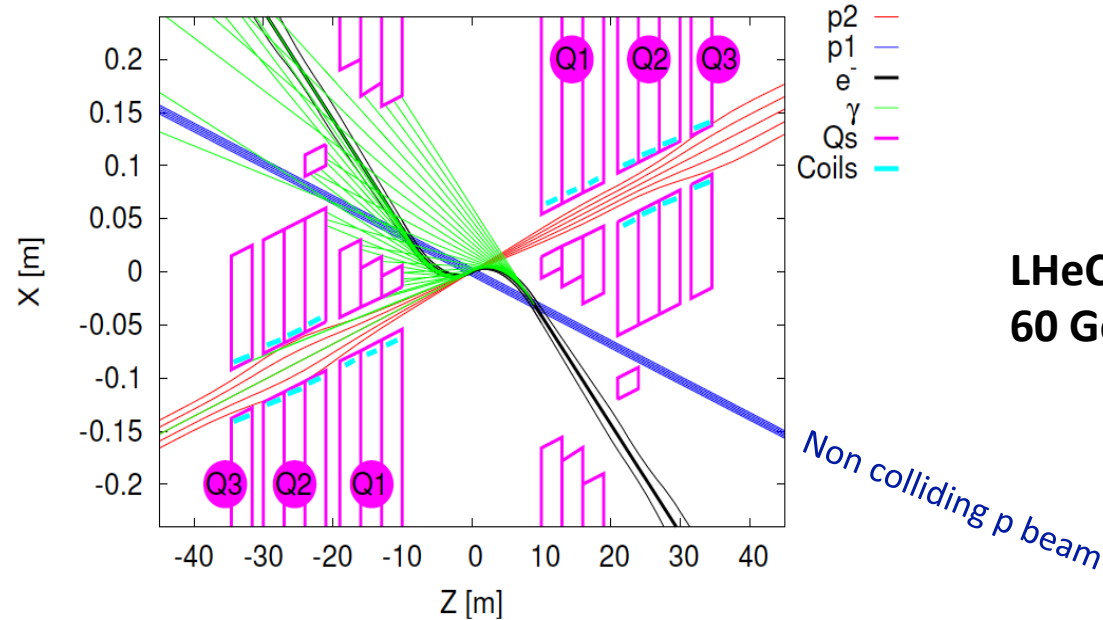
Dimensions and Multitudes – FCC-eh

Tracker	FST _{pix}	FST _{striz}	CFT _{pix}	CPT _{pix}	CST _{striz}	CBT _{pix}	BST _{striz}	BST _{pix}
#Wheels	7		2	–	–	2	5	
#Rings/Wheel	2 _{inner}	3 _{outer}	3/4	–	–	3/4	3 _{outer}	2 _{inner}
#Layers	–	–	–	4	5	–	–	–
$\theta_{min/max}$ [°]	0.5	3.8	3.6	5.1	24/155	176.4	173.1	179.3
$\eta_{max/min}$	5.4	3.4	3.5	±3.1	±1.4	-3.5	-2.8	-5.2
Si _{pix/striz} [m ²]	9.7	13.3	2.8	5.4	33.7	2.8	9.7	6.9
Sum-Si [m ²]	84.3 double layers taken into account							
Calo	FHC _{SiW}	FEC _{SiW}	EMC _{SciPb/LAr}		HAC _{SciFe}		BEC _{SiPb}	BHC _{SiFe}
$\theta_{min/max}$ [°]	0.3	0.4	5.6/173.4		8.6/167		179.4	179.6
$\eta_{max/min}$	6.0	5.6	3.0/-2.7		2.5/-2.2		-5.3	-5.6
Volume [m ³]	13.2	3.1	28.8		407		1.98	7.0
Sum-Si [m ²]	461							

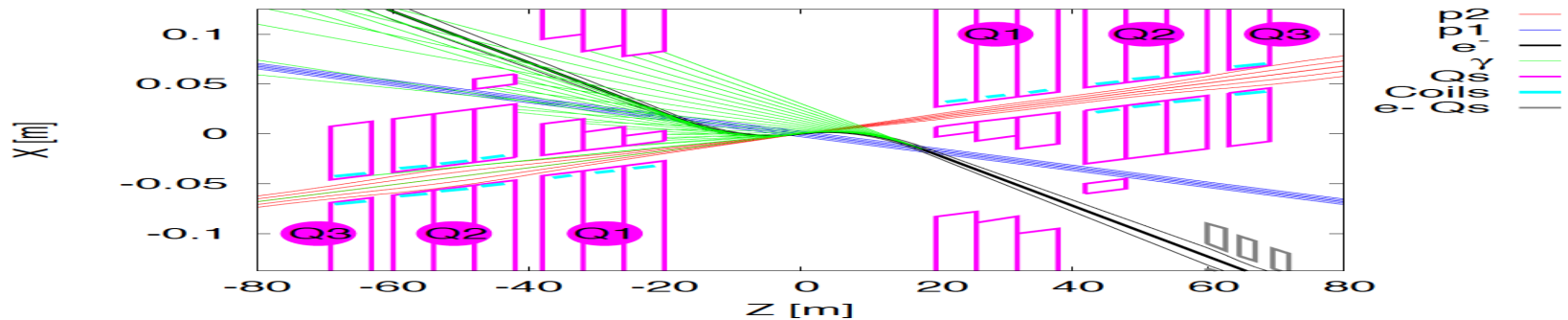
Interaction Regions for ep with Synchronous pp Operation



Still work in progress:
may not need half
quad if $L^*(e) < L^*(p)$



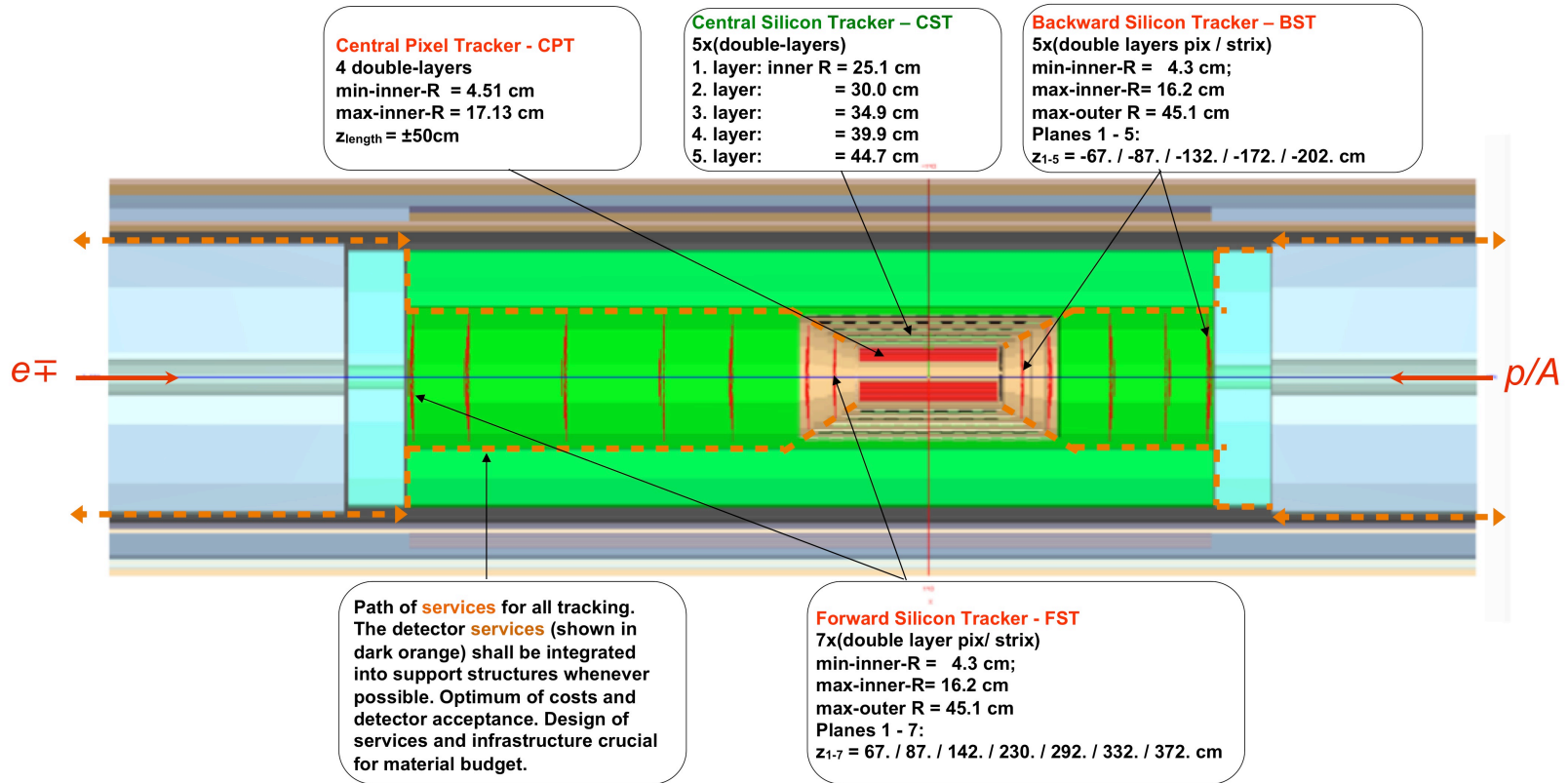
LHeC (CDR)
60 GeV * 7 TeV



FCC-he (ERL)
60 GeV * 50 TeV

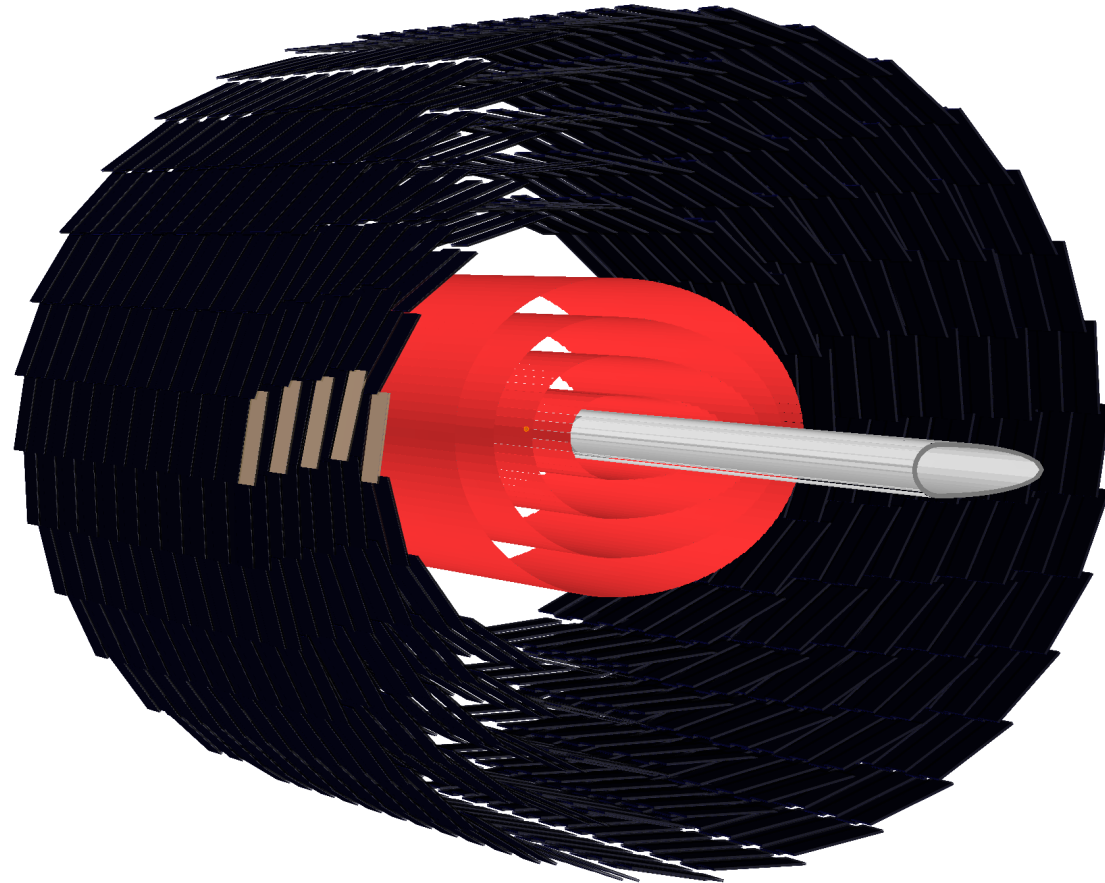
Tentative: $\epsilon_p = 2\mu\text{m}$, $\beta^* = 20\text{cm} \rightarrow \sigma_p = 3\mu\text{m} \approx \sigma_e$ matched! $\epsilon_e = 5\mu\text{m}$..

Detector design: Inner Silicon Tracker (status 3/16)

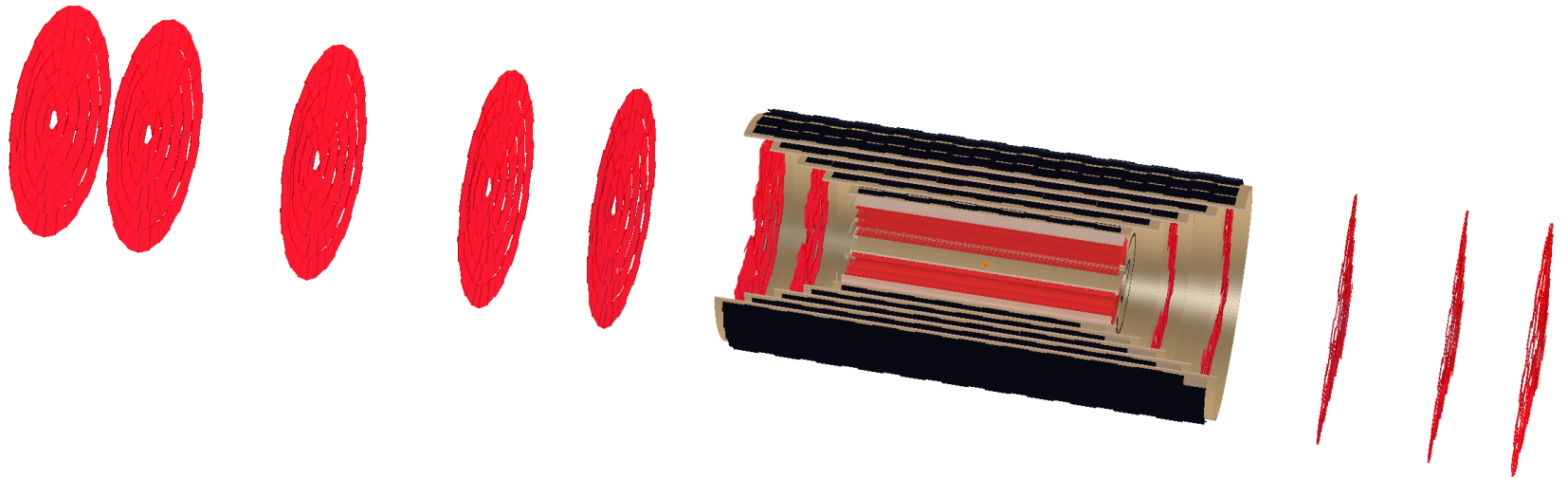


More detailed designs for other components too. DD4HEP software developments..
 An opportunity for R+D and building a novel, challenging 4π detector in the twenties.
Profit from HL LHC detector upgrades, also ILC, with no pileup and small radiation load

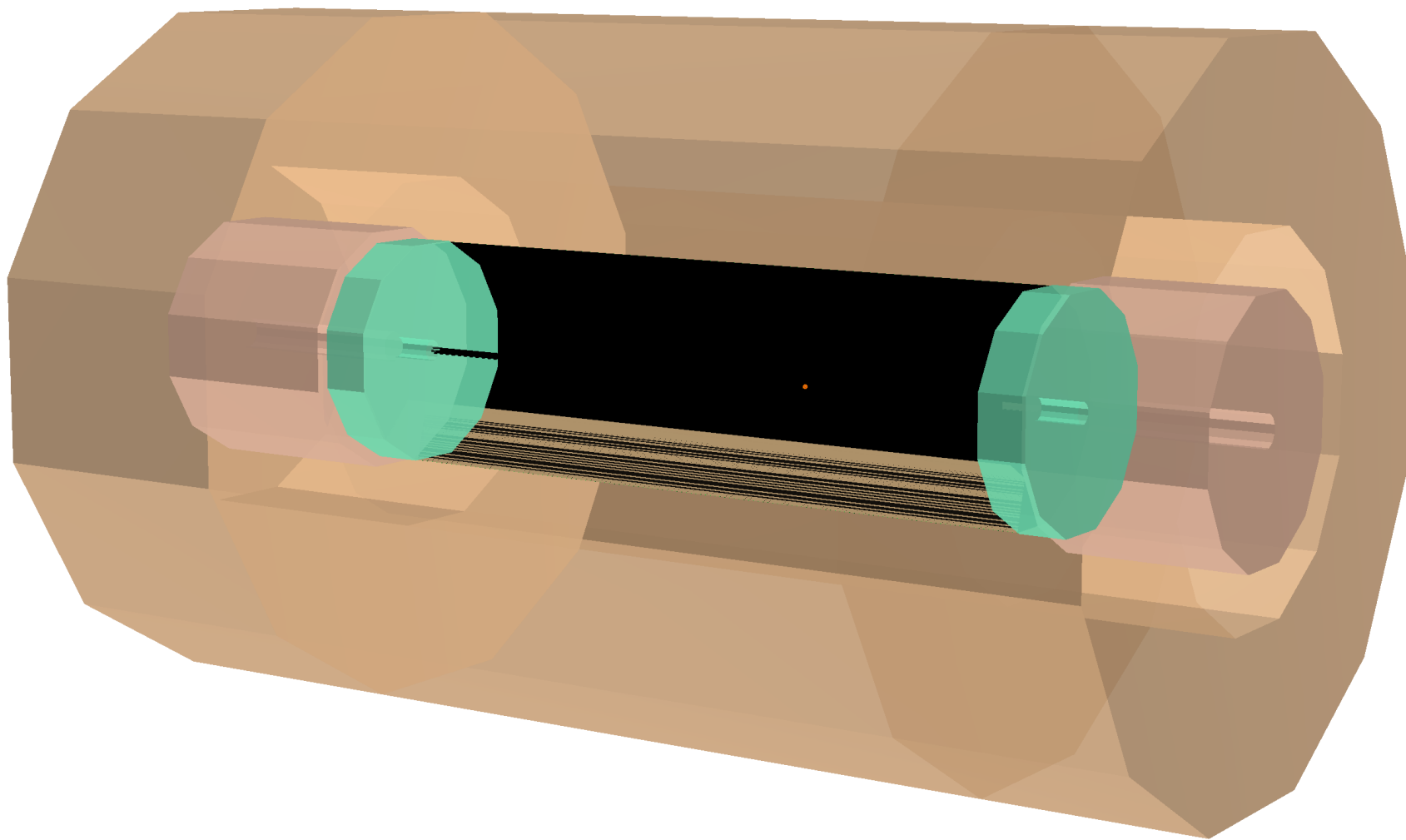
LHeC Silicon Tracker



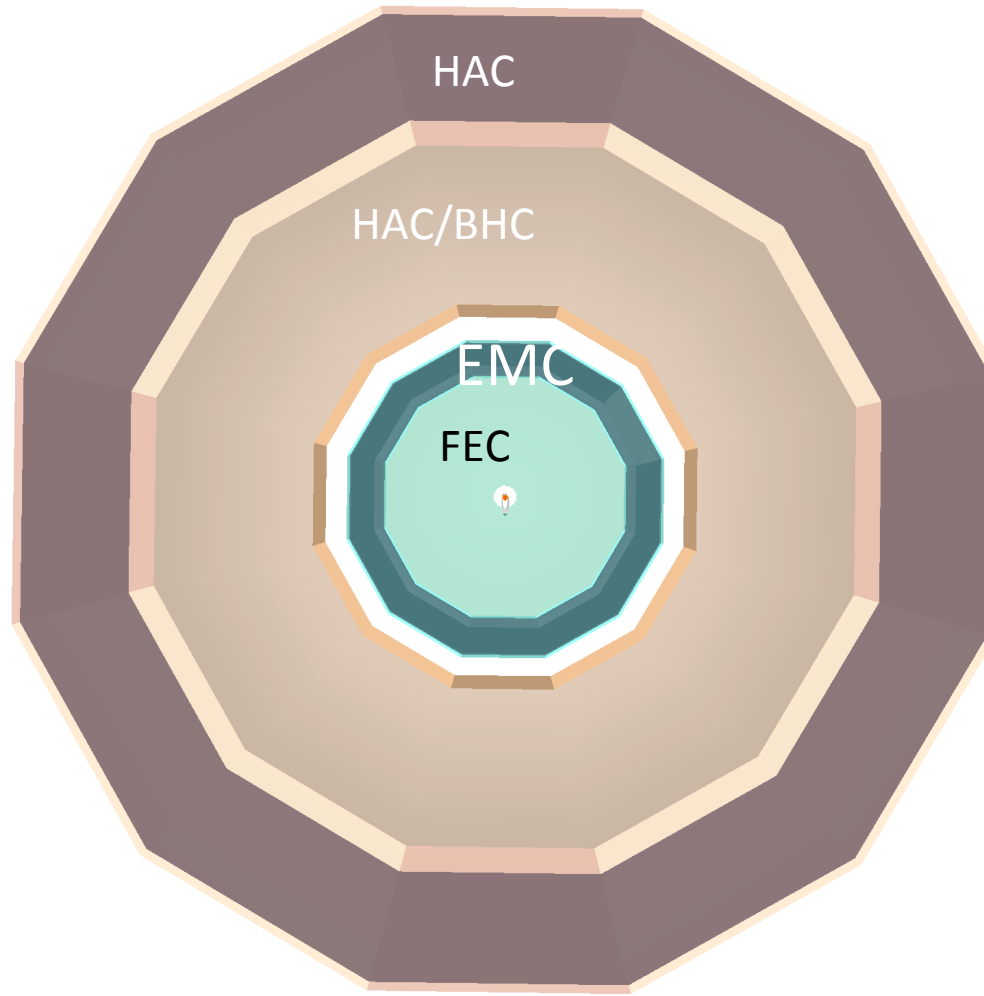
The LHeC Silicon Tracker



LHeC Calorimeters



Cut through Calorimeters at $z=510\text{cm}$



Outer radius: 3.6m

Software Status

Software based on DD4hep/DDG4 - pre-release software [AIDAsoft/DD4hep];
Python, C++

LHeC/FCC detector geometry, material description, R/O description as needed,
segmentations and surfaces - ingredients for reconstruction;

DDEve - event display tool for quality judgment and control ...

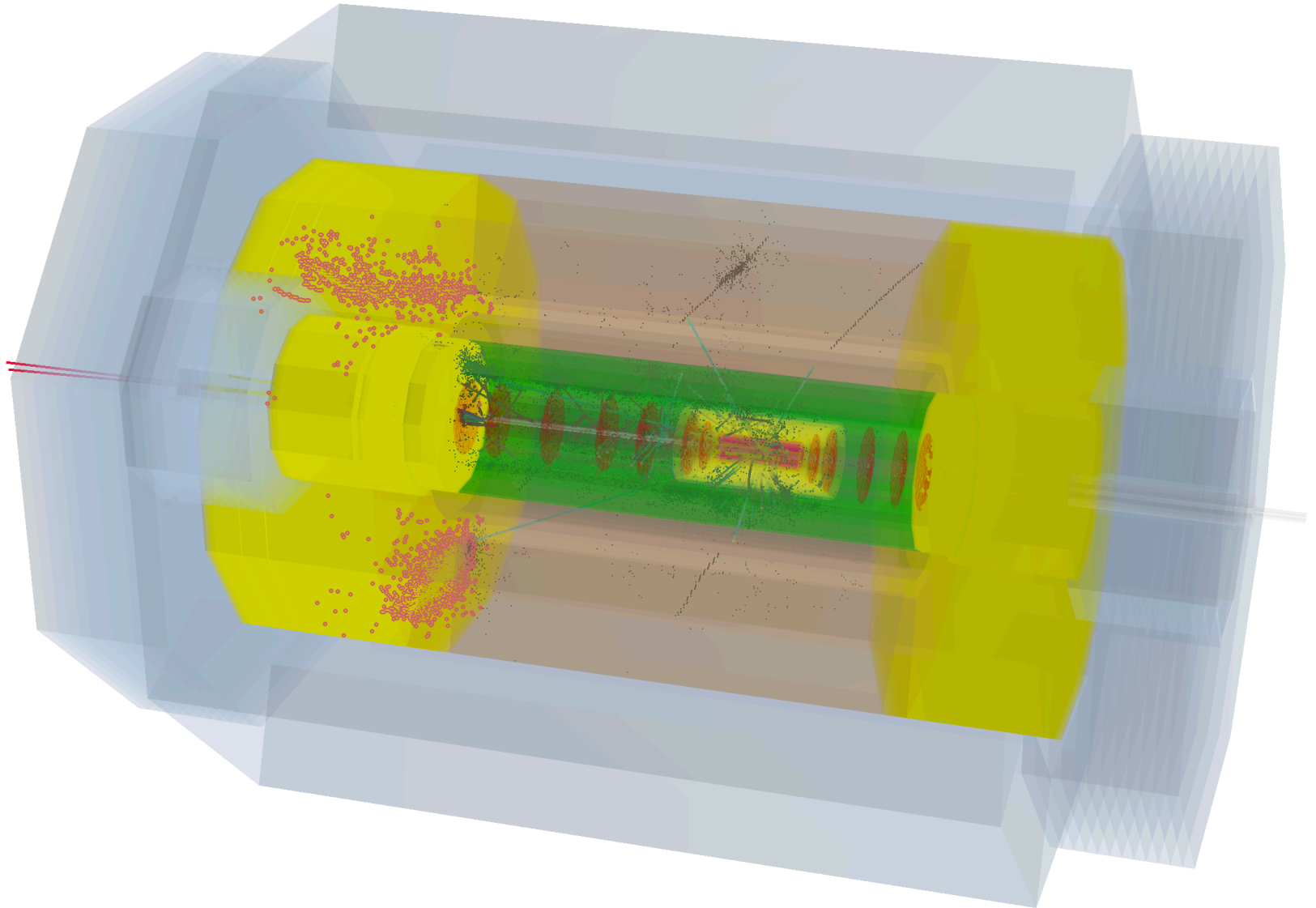
Follow the main developments & build a detector model answering physics
questions (reuse of experience and implementations)

Collaboration inside the FCC-Software effort at CERN - information @ [http://
fccsw.web.cern.ch/fccsw/](http://fccsw.web.cern.ch/fccsw/)

Synergies when following closer the FCC-SW initiative - new EDM, geometry/
material definitions based on DD4hep as well, using GAUDI for overall steering;
aspects of commonly used tracking software (ACTS); fast and detailed
simulation

Hardware optimisation according to latest R&D (HL-LHC ...)

$H \rightarrow b\bar{b}$ in LHeC Detector





Next Steps



Interaction region update

Finish ep Detector software link to Higgs, top, PDF.. physics study

Technology choices for novel, high tech, high precision detector post HL-LHC

CDR for FCC-eh Detector (I/2018)

Update of LHeC Detector Design (IV/2018) – will include cost-energy-physics study

Many thanks to

**Andrea Gaddi, Hermann ten Kate, Peter Kostka, Ercan Pilcer,
Brett Parker, Alessandro Polini, Stefan Russenschuck, RogelioTomas and many others**

title

